12th ANKARA INTERNATIONAL AEROSPACE CONFERENCE **AIAC-2023-043**
13-15 September 2023 - Online, Ankara, TURKEY

A CONTROL STRATEGY FOR THE POWERED LANDING OF A REUSABLE ROCKET BOOSTER

Amr Elsherbiny* and Anna Prach†
Middle East Technical University
Northern Cyprus Campus

ABSTRACT

This paper presents the control system for a reusable rocket booster during the final stage of the powered-landing phase. The controller consists of three control channels each featuring a multiple-loop structure. The goal of the controller is to provide accurate tracking of the desired altitude, minimize the horizontal displacement, and stabilize the angular position of the booster. Numerical simulations are carried out using a 3 DOF nonlinear model of the rocket booster.

INTRODUCTION

Reusable launch vehicles provide the most effective way to reduce the cost of the space transportation. One of the main challenges in the reusable space rocket technology is landing of the rocket or its parts such as boosters. Private companies such as SpaceX and Blue Origin have demonstrated successful vertical landing of reusable boosters [Blackmore, 2016]. This task requires recovery guidance navigation and control (GNC) strategy and algorithms, which is particular challenging task for the powered-landing phase. A GNC algorithm must enable precise landing with low fuel margins and significant dispersions. The state-of-the-art solutions for navigation and control problems have been proposed within the frameworks of hybrid navigation techniques and robust control. For the powered descent guidance problem novel techniques are required to enable on-board optimization, that is necessary to achieve the landing accuracy required to recover the rocket boosters.

Various GNC algorithms have been proposed for the powered descent problem applications, among which optimization-based techniques are the most explored [Acikmese and Ploen, 2005, 2007; Najson and Mease, 2005; Ganet-Schoeller and Brunel, 2019; Malyuta et al., 2019; Wang et al., 2019; Botelho et al., 2022]. Model predictive control [Zaragoza Prous, 2020; Guadagnini et al., 2022] is given a lot of attention since it allows to take into account the state and control constraints while solving the optimization problem.

A common idea for the optimization is to determine a fuel-optimal trajectory and the actuators demands necessary to follow this trajectory. The computational cost is an important consideration since the solver must find a feasible solution in a fraction of a second in real time.

This paper focuses on the control the rocket booster during the final landing phase and the touch-

*Graduate Student, Email: elsherbiny.amr@metu.edu.tr
†Assist. Prof. Dr. in Aerospace Engineering Department, Email: aprach@metu.edu.tr

down. The booster is located above the landing pad, and is guided vertically downward. A vertical position profile is defined such that it will have a constant descent rate for most of the landing phase, with a decreasing descent rate right before the touchdown.The vertical position control is achieved by adjusting the magnitude of the thrust. The horizontal displacement is controlled using both the thrust vectoring and the side force. At the same time, stabilization of the angular motion is provided by the controller that uses the side jet thrusters to keep the booster aligned vertically during landing. A classical control method is applied implementing a multi-loop controller architecture featuring proportional and derivative (PD) controllers. The system has three independent control inputs including the magnitude of the main engine's thrust, the direction of the main engine's thrust (thrust vectoring), and the magnitude and the direction of the side thrusters force. The control allocation is described in the controller structure section of the paper. The numerical study is carried out for several simulation scenarios to test and validate the proposed control algorithms using a nonlinear simulation model of the rocket booster. The paper is organized as follows. Problem statement and literature review are presented in the Introduction section. Next section covers the description of the mathematical model of the booster. The controller structure is given in the next section, and followed by the numerical simulation results and the conclusions.

METHODOLOGY

Mathematical Modelling of the Booster

The mathematical model of the booster uses 3DOF rigid body dynamics, which describes the position and attitude, as shown in Fig. 1. The forces acting on the booster include weight, the aerodynamic forces, the main engine thrust, and the reaction control system (RCS) force which uses the cold gas Draco thrusters located at the top part of the booster.

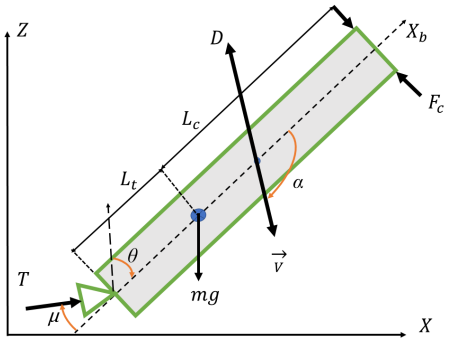

Figure 1: The 3 DOF dynamic model of the booster

The translational and rotational equations of motion are given by

$$m(t)\ddot{x} = Tsin(\theta + \mu) + F_c cos(\theta) + F_x, \tag{1}$$

$$m(t)\ddot{z} = Tcos(\theta + \mu) - F_c sin(\theta) - m(t)g + F_z, \tag{2}$$

$$J\ddot{\theta} = Tsin(\mu)l_t + F_c l_c - F_z x_s, \tag{3}$$

where $m(t)$ is the mass of the booster, J is the moment of inertia of the booster, T is the engine thrust, F_c represents the RCS force, μ and θ are the gimbal and pitch angles, respectively. F_x, F_z are the aerodynamic forces acting in the x and z directions, respectively. x_s represents the distance between the aerodynamic center and the center of gravity $(c.g)$ of the booster. F_x and F_z are calculated by transforming the aerodynamic forces from the wind frame into the inertial frame.

The mass of the booster changes according to the fuel mass flow rate

$$m = m_0 - \frac{1}{I_{sp}} \int T_t \, dt \;, \dot{m} = -\frac{T_t}{I_{sp} \cdot g_0}, \tag{4}$$

where m_0 is the initial mass at the moment of initiation of the landing maneuver, I_{sp} is the specific thrust, T_t is the total thrust effort, and g_0 is the gravitational constant. The aerodynamic drag is calculated as

$$D = 0.5\rho V^2 S(\alpha) C_D(\alpha, M), \tag{5}$$

where ρ is the atmospheric air density which assumed to be constant, V is the air velocity. C_D represents the drag coefficient of the booster, and is a function of the angle of attack α and the Mach number M. The reference area S is a function of the angle of attack α, and is given by

$$S(\alpha) = 2\pi R l sin(\alpha) + \pi R^2 cos(\alpha), \tag{6}$$

where R is the radius of the booster and l is the length. The angle of attack α is determined from

$$\alpha = 90 - |\theta| + \gamma, \tag{7}$$

where $\gamma = atan(\frac{\dot{z}}{\dot{x}})$, $\dot{z}$ and $\dot{x}$ are the velocities of the rocket with respect to the landing point in z and x directions, respectively. The aerodynamic forces are defined with respect to the air-trajectory reference frame w

$$\begin{pmatrix} {F_x}^w \\ {F_z}^w \end{pmatrix} = \begin{pmatrix} -D \\ 0 \end{pmatrix}, \tag{8}$$

$$\begin{pmatrix} {F_x}^i \\ {F_z}^i \end{pmatrix} = \begin{pmatrix} -Dcos(\gamma) \\ Dsin(\gamma) \end{pmatrix}. \tag{9}$$

Controller Structure

To achieve precise position control and stabilization during the final landing phase, a multiple-loop controller structure is introduced. The controller structure is shown in Fig. 2. Three parallel control channels yield three control inputs including thrust magnitude, gimbal angle, and the force of the side thrusters. Each control channel features a dual-loop structure that uses the motion variable and its derivative in the feedback. This allows to increase the accuracy and gives more flexibility when tuning the controllers gains.

In the first control channel, two PD controllers, PD_1 and PD_2 are used to control the vertical descent and descent rate using the main engine thrust. PD_3 and PD_4 are used in the second channel to stabilize the pitch angle and the pitch rate using the vectored thrust via adjusting the gimbal angle. The horizontal displacement is controlled by the third channel via PD_5 and PD_6 controllers that yield the RCS demands. The actuators are modeled as a first order dynamic systems. The values of the PD controllers' gains are given in Table 1.

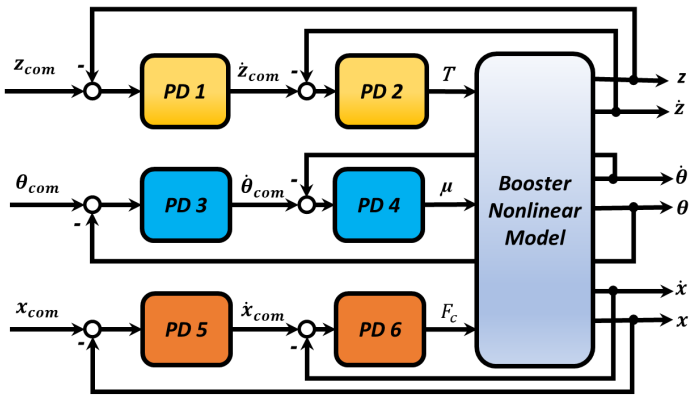

Figure 2: Z, θ, and X Controllers Structure

Gain \ Controller	PD_1	PD_2	PD_3	PD_4	PD_5	PD_6
K_p	1.1	$25 \cdot 10^3$	7	-0.1	0.2	$-2 \cdot 10^3$
K_d	0	0	0.1	0	0.1	0

Table 1: PD controllers gains

RESULTS AND DISCUSSION

Numerical simulations are carried out using a nonlinear simulation model of the booster. The booster specification is given in Table 2.

Parameter	Value	Unit
m_0	22000	kg
mf	6000	kg
T	$0 \geq T \leq 3 * 845$	kN
F_c	$-5000 \geq F_c \leq 5000$	N
l_t	17.7	m
l_c	27.6	m
μ	$-25 \geq \mu \leq 25$	deg
J_0	$5 * 10^5$	$kg \cdot m^2$
R	3.6	m
x_s	4.95	m
C_D	$0.5 \geq C_D \leq 2$	

Table 2: The parameters of Falcon 9 V.5 Booster [SPACEX, 2023; Prous, 2020].

Case 1: Landing

The landing manuever is initiated when the booster's altitude is 100 m above the ground with a vertical downward speed equal to 10 m/s. The horizontal displacement at the initial time instant is 10 m, and the horizontal velocity is equal to 5 m/s, the initial angular displacement is 20 deg, and the initial angular rate is 0 deg/s. Figures 3 and 7 show the corresponding responses for the vertical and horizontal positions and velocities respectively. Figure 4 shows the responses of the pitch angle, and the corresponding control inputs that is the gimbal angle, the thrust and the RCS are shown in Fig.6.Time variation of the mass is shown in Fig.5. The simulation shows accurate responses to stabilize the system with touchdown velocities of less than 0.5 m/s in both horizontal and vertical directions.

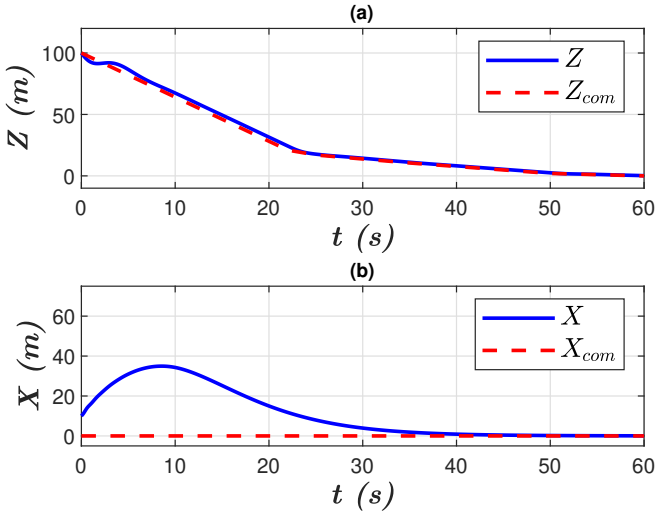

Figure 3: Case 1: (a) vertical displacement, (b) horizontal displacement

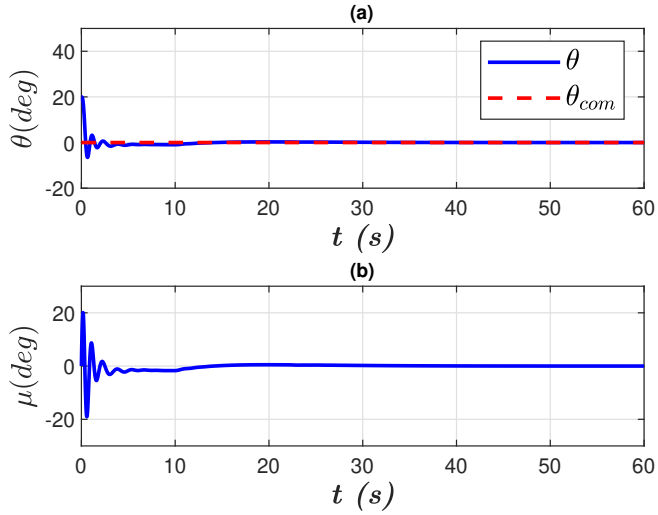

Figure 4: Case:1 (a) Pitch angle. (b) Gimbal angle

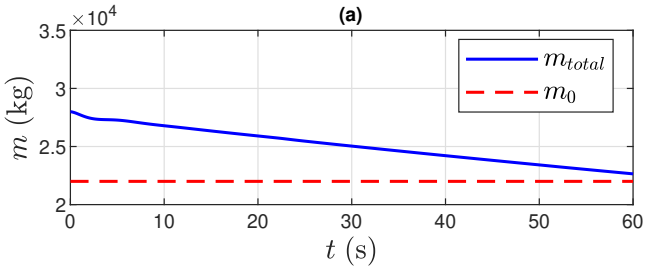

Figure 5: Case 1: Mass change with thrust per time

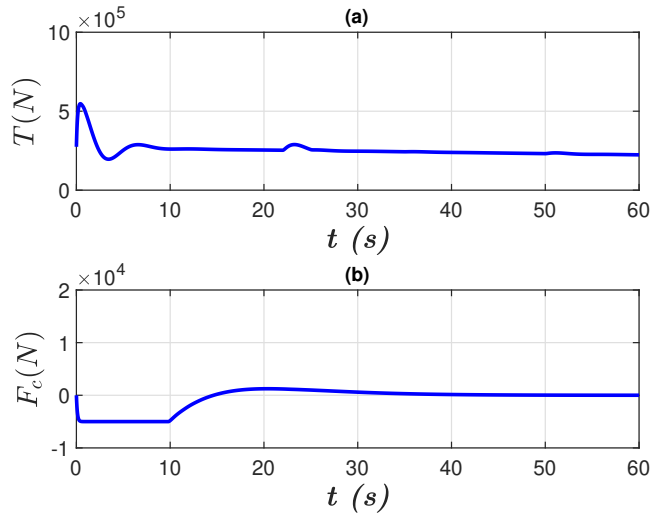

Figure 6: Case 1: (a) Thrust input. (b) Side force input

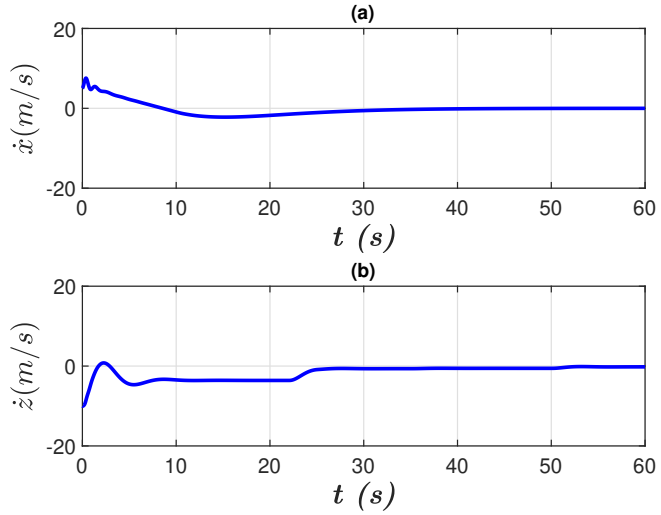

Figure 7: Case 1: (a) Vertical velocity. (b) Horizontal velocity

Case 2: Flip maneuver and landing

In this simulation scenario, the booster is falling down horizontally, i.e. $\theta = 90$ deg at 100 m altitude with a vertical downward velocity equal to 10 m/s. A flip maneuver is required first to bring the booster to the vertical orientation for landing. The initial horizontal displacement and velocity are 10 m and 5 m/s, respectively. The simulation results are given in Figures 8-10, where figures 8 and 12 show the corresponding responses for the vertical and horizontal positions and velocities, and Fig. 9 shows the responses of the pitch angle, and the corresponding control inputs that is the gimbal angle, the thrust and the RCS are shown in Fig.11. Figure 10 shows the variation of the mass of the booster. The simulation results illustrate successful execution of the flip maneuver, and stabilization of the pitch angle.

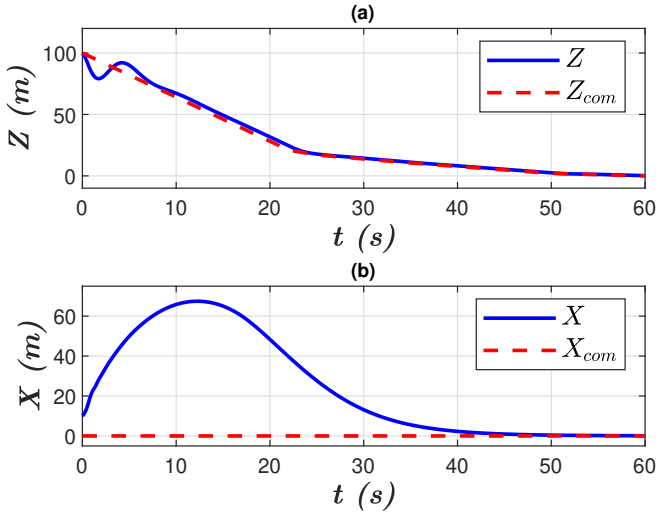

Figure 8: Case 2: (a) vertical displacement, (b) horizontal displacement

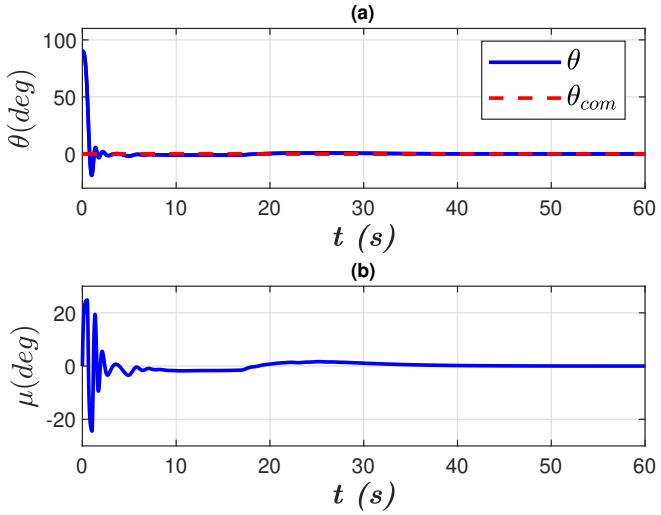

Figure 9: Case:2 (a) Pitch angle. (b) Gimbal angle

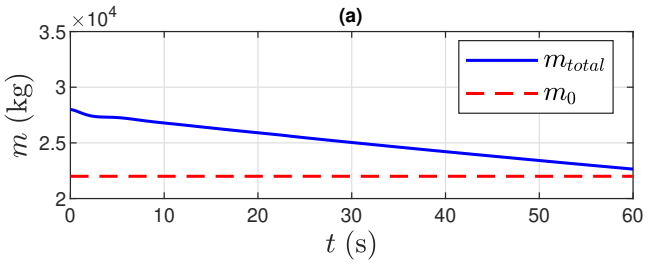

Figure 10: Case 2: Mass change with thrust per time

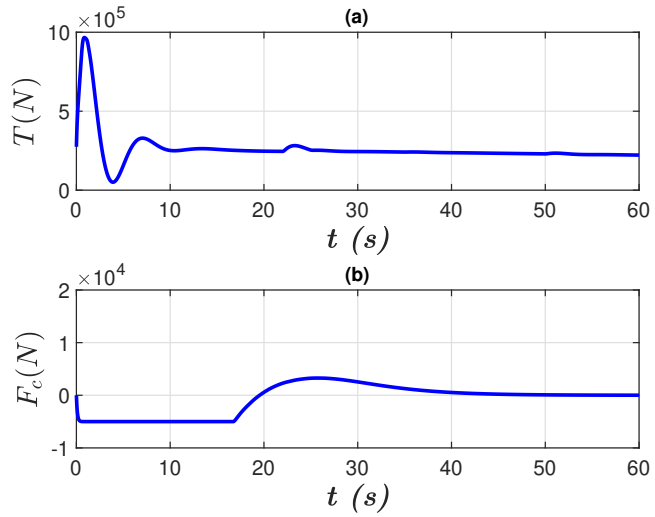

Figure 11: Case 2: (a) Thrust input. (b) Side force input

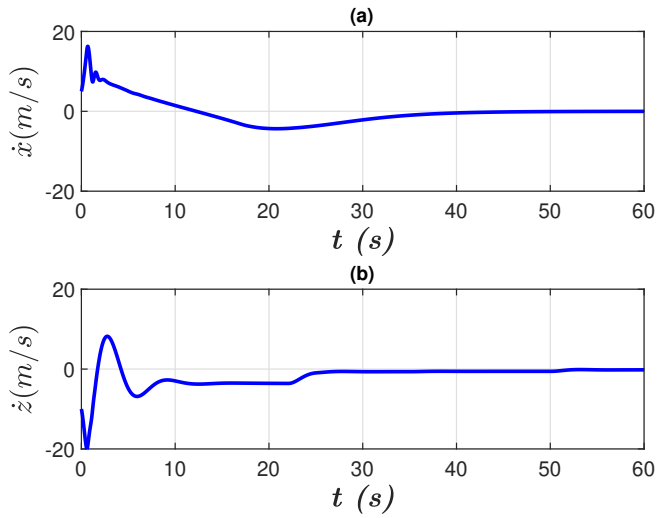

Figure 12: Case 2: (a) Vertical velocity. (b) Horizontal velocity

Case 3: Flip maneuver and landing with wing gust

In this simulation scenario, the booster is falling down horizontally, i.e. $\theta = 90$ deg at 100 m altitude with a vertical downward velocity equal to 10 m/s. Besides, a vertical and horizontal wind gust are applied to the booster with magnitude and time as shown in Fig.13. The flip maneuver is required first to bring the booster to the vertical orientation for landing and withstanding the required landing conditions at the vertical and horizontal gusts. The initial horizontal displacement and velocity are 10 m and 5 m/s, respectively. The simulation results are given in figures 14-15, where figures14 and 18 show the corresponding responses for the vertical and horizontal positions and velocities, Fig.16 shows the responses of the pitch angle, and the corresponding control inputs that is the gimbal angle, the thrust and the RCS force are shown in Fig.17. Figure 15 shows the mass variation of the booster.

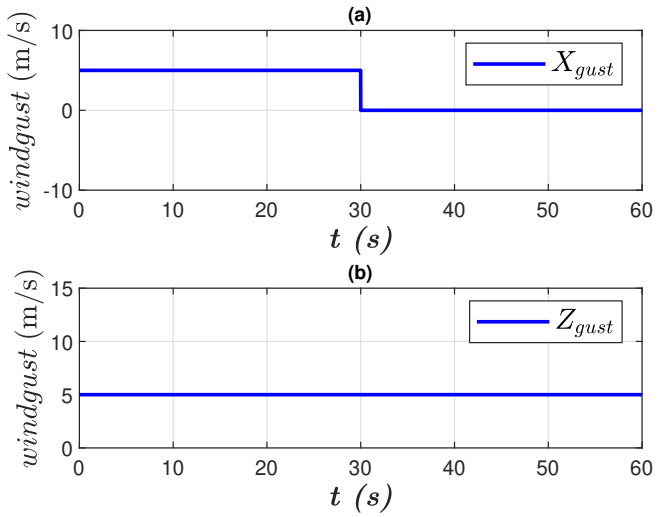

Figure 13: Case 3: (a) Horizontal gust, (b) vertical gust

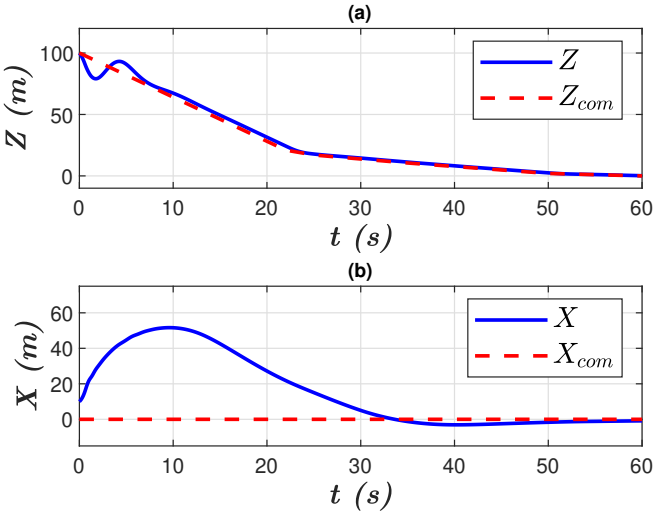

Figure 14: Case 3: (a) vertical displacement, (b) horizontal displacement

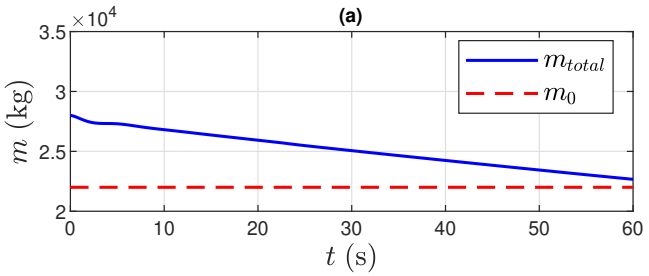

Figure 15: Case 2: Mass change with thrust per time

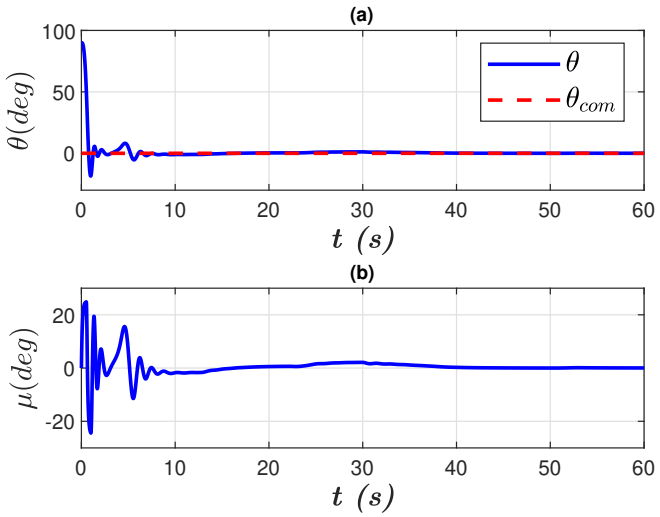

Figure 16: Case:3 (a) Pitch angle. (b) Gimbal angle

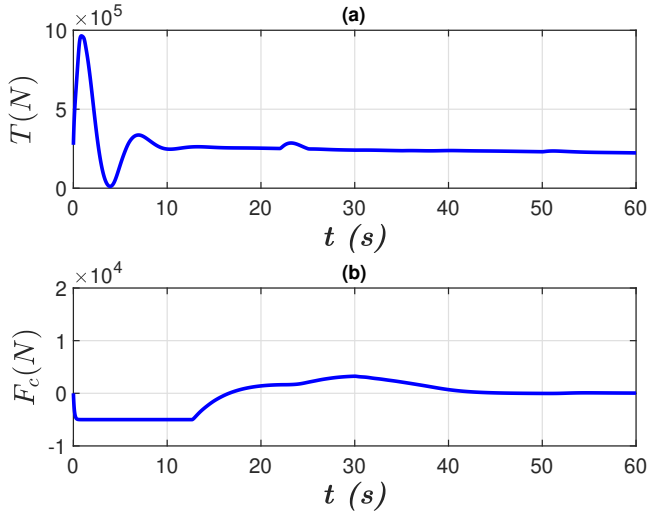

Figure 17: Case 3: (a) Thrust input. (b) Side force input

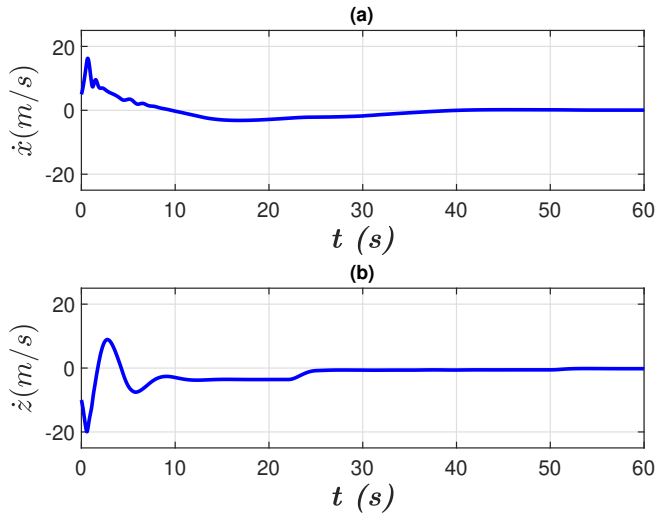

Figure 18: Case 3: (a) Vertical velocity. (b) Horizontal velocity

CONCLUSIONS

This paper presents a controller for a reusable rocket booster landing. The aim of the controller is to provide tracking of the desired altitude profile, stabilize the angular motion of the booster, and minimize the horizontal displacement with respect to the landing pad. The controller structure consists of several control channels featuring PD controllers, providing the three control inputs including the main engine thrust, the gimbal angle, and the RCS. The performance of the controller is validated via numerical simulations utilizing a nonlinear dynamic model of the booster with time varying mass. The proposed controller is tested for various landing scenarios including the landing with a flip maneuver, and landing in the presence of atmospheric disturbances. The results illustrate the effectiveness of the proposed controller to provide accurate command following and stabilization of the rocket booster.

References

Acikmese, B. and Ploen, S. R. (2005). A Powered Descent Guidance Algorithm for Mars Pinpoint Landing | Guidance, Navigation, and Control and Co-located Conferences. [Online; accessed 10. Mar. 2023].

Acikmese, B. and Ploen, S. R. (2007). Convex programming approach to powered descent guidance for mars landing. *Journal of Guidance, Control, and Dynamics*, 30(5):1353–1366.

Blackmore, L. (2016). Autonomous precision landing of space rockets. 46:15–20.

Botelho, A., Martinez, M., Recupero, C., Fabrizi, A., and De Zaiacomo, G. (2022). Design of the landing guidance for the retro-propulsive vertical landing of a reusable rocket stage. *CEAS Space Journal*, 14(3):551–564.

Ganet-Schoeller, M. and Brunel, A. (2019). Optimal guidance for 1st stage launcher recovery. *IFAC-PapersOnLine*, 52:532–537.

Guadagnini, J., Lavagna, M., and Rosa, P. (2022). Model predictive control for reusable space launcher guidance improvement. *Acta Astronautica*, 193:767–778.

Malyuta, D., Reynolds, T., Szmuk, M., Mesbahi, M., Açıkmeşe, B., and Carson, J. (2019). Discretization performance and accuracy analysis for the rocket powered descent guidance problem.

Najson, F. and Mease, K. (2005). *A Computationally Non-Expensive Guidance Algorithm for Fuel Efficient Soft Landing*.

Prous, G. Z. (2020). Guidance and control for launch and vertical descend of reusable launchers using model predictive control and convex optimisation.

SPACEX (2023). Space x falcon's user guide. https://https://www.spacex.com/vehicles/falcon-9/.

Wang, J., Cui, N., and Wei, C. (2019). Optimal rocket landing guidance using convex optimization and model predictive control. *Journal of Guidance, Control, and Dynamics*.

Zaragoza Prous, G. (2020). Guidance and control for launch and vertical descend of reusable launchers using model predictive control and convex optimisation. Space engineering, master's level (120 credits), Luleå University of Technology, Department of Computer Science, Electrical and Space Engineering.